Computers and Concrete, *Vol. 25, No. 6 (2020) 575-585*
DOI: https://doi.org/10.12989/cac.2020.25.6.575

Assessment of transient vibrations of graphene oxide reinforced plates under pulse loads using finite strip method

Seyed Sajad Mirjavadi[1], Masoud Forsat*[2], Mohammad Reza Barati[3] and A.M.S. Hamouda[1]

[1]*Department of Mechanical and Industrial Engineering, Qatar University, P.O. Box 2713, Doha, Qatar*
[2]*Department of Civil and Architectural Engineering, Qatar University, Doha, Qatar*
[3]*Fidar Project Qaem Company, Darvazeh Dolat, Tehran, Iran*

(*Received March 25, 2020, Revised May 18, 2020, Accepted May 26, 2020*)

Abstract. Based on a refined shear deformation finite strip, transient vibrations of graphene oxide powder (GOP) reinforced plates due to external pulse loads have been investigated. The plate has uniformly and linearly distributed GOPs inside material structure. Applied pulse loads have been selected as sinusoidal, linear and blast types. Such pulse loads result in transient vibrations of the GOP-reinforced plates which are not explored before. Finite strip method (FSM) has been performed for solving the equations of motion and then inverse Laplace transform technique has been employed to derive transient responses due to pulse loading. It is reported in this study that the transient responses of GOP-reinforced plates are dependent on GOP dispersions, GOP volume fraction, type of pulse loading, loading time and load locations.

Keywords: transient response; vibration; graphene oxide powder; concrete plate; finite strip; pulse load

1. Introduction

Based on recent knowledge, different carbon structures including carbon nanotube and carbon fiber are extensively applied in composite materials to enhance their thermal and mechanical characteristics (Zhang 2017, Keleshtreri *et al*. 2016, Mirjavadi *et al*. 2017, 2018, 2019, Azimi *et al*. 2017, 2018). An increase of about 273% in elastic moduli of a carbon reinforced composite compared with a traditional composite has been reported by Ahankari *et al*. (2010). Also, Gojny *et al*. (2004) stated that the stiffness of carbon reinforced composite can be increased even by embedding a small amount of carbon nanotube. The effects of shape and size of carbon nanotubes on stiffness enhancement of composite materials with metal matrix have been investigated by Esawi *et al*. (2011). Due to having such superior characteristics, structural elements (beams and plates) with embedded carbon nanotubes have been investigated in the view of their static and dynamical properties (Yang *et al*. 2017). However, graphene reinforced composites have been recently attracted huge attention due to their easier production approach and excellent stiffness enhancement mechanism. A review of different graphene nanoplate reinforced composites having ceramic and metal matrices has been represented by Nieto *et al*. (2017). A multi-scale analysis of mechanical characteristics of graphene nanoplate reinforced composites is presented by Lin *et al*. (2018) using finite element method.

Until now, many of researches in the fields of nano-composites have been interested in production and materials characteristics recognition of graphene based composites and structural components containing slight percentages of graphene fillers. For instance, it is mentioned by Rafiee *et al*. (2009) that some material characteristics of graphene based composites may be enhanced via placing 0.1% volume of graphene filler. However, achieving to this level of reinforcement employing nanotubes required 1% of their volume. Graphene based composites containing epoxy matrix were created by King *et al*. (2013) by placing 6% weight fraction of graphene fillers to polymeric phases. It was stated that Young modulus of the composite has been increased from 2.72 GPa to 3.36 GPa. Next, 57% increment for Young modulus has been achieved by Fang *et al*. (2009) based on a sample of graphene based composite.

Moreover, many studies in the fields of nano-mechanic are associated with vibrational and stability investigation of various structural elements containing beam or plate reinforced via diverse graphene dispersions. For instance, vibrational properties of a laminated graphene based plate have been explored by Song *et al*. (2017) assuming simply support edge condition. They assumed that the plate is constructed from particular numbers of layers each containing a sensible content of graphene. Selecting a perturbation approach, static deflections and bucking loads of graphene based plates have been derived by Shen *et al*. (2017). In above papers, each material property has discontinuous variation across the thickness of beam or plate. Also, geometrically nonlinear vibration frequencies of graphene based beams having embedded graphene have been explored by Feng *et al*. (2017) selecting first-order beam theory. Moreover, vibration frequencies of graphene based beams having porosities have been explored by Kitipornchai *et al*. (2017).

*Corresponding author, Ph.D.
E-mail: masoudforsatlar@gmail.com

ISSN: 1598-8198 (Print), 1598-818X (Online)

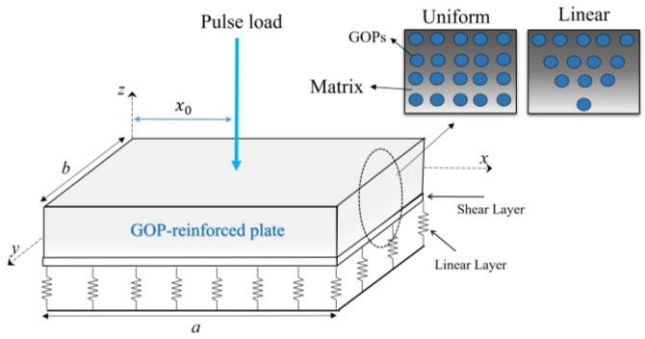

Fig. 1 A GOP-reinforced plate under a pulse loading

Recently, reinforcement of concrete with nano-size inclusions is a novel case study. Many researches show that mechanical properties of concrete can be enhanced by adding graphene platelets (GPLs), graphene oxide powders (GOPs) and ever carbon nanotubes (Du *et al*. 2016, Shamsaei *et al*. 2018). Graphene oxide, a derivative of graphene, is extensively and economically available from graphite mass oxidations. It is compatible with many matrix materials including polymeric materials and even concrete (Mohammed *et al*. 2017). Composites of graphene oxide display excellent Young modulus and tensile strengths as are carbon-based materials with low cost and prominent performances (Zhang *et al*. 2020). To the best of author's knowledge, transient vibration study of concrete plates reinforced by GOPs under pulse loads is not performed yet.

Based on a refined shear deformation finite strip, transient vibrations of graphene oxide powder (GOP) reinforced plates due to external pulse loads have been investigated. The plate has uniformly and linearly distributed GOPs inside material structure. Applied pulse loads have been selected as sinusoidal, linear and blast types. Such pulse loads result in transient vibrations of the GOP-reinforced plates which are not explored before. Finite strip method (FSM) has been performed for solving the equations of motion and then inverse Laplace transform technique has been employed to derive transient responses due to pulse loading. It is reported in this study that the transient responses of GOP-reinforced plates are dependent on GOP dispersions, GOP volume fraction, type of pulse loading, loading time and load locations.

2. GOP-based composites

According to Fig. 1, it is assumed that GOPs have two types of dispersion within the structure including uniform-type and linear-type. In this figure, a GOP reinforced composite plate is illustrated. Micro-mechanic theory of such composite materials (Liew *et al*. 2015, Medani *et al*. 2019, Zarga *et al*. 2019) introduces the below relationship between GOPs weight fraction (W_{GOP}) and their volume fraction (V_{GOP}) by

$$V_{GOP}^{*}=\frac{W_{GOP}}{W_{GOP}+\frac{\rho_{GOP}}{\rho_M}-\frac{\rho_{GOP}}{\rho_M}W_{GOP}} \tag{1}$$

where ρ_{GOP} and ρ_M define the mass densities of GOP and matrices, respectively. Next, the elastic modulus of a GOP based composite might be represented based upon matrix elastic modulus (E_M) by (Zhang *et al*. 2020)

$$\begin{aligned}E_1=0.49&\left(\frac{1+\xi_L^{GOP}\eta_L^{GOP}V_{GOP}}{1-\eta_L^{GOP}V_{GOP}}\right)E_M\\&+0.51\left(\frac{1+\xi_W^{GOP}\eta_W^{GOP}V_{GOP}}{1-\eta_W^{GOP}V_{GOP}}\right)E_M\end{aligned} \tag{2}$$

so that ξ_L^{GOP} and ξ_W^{GOP} define two geometrical factors indicating the impacts of graphene configuration and scales as

$$\xi_L^{GOP}=\frac{2d_{GOP}}{t_{GOP}} \tag{3a}$$

$$\eta_L^{GOP}=\frac{\left(E_{GOP}/E_M\right)-1}{\left(E_{GOP}/E_M\right)+\xi_L^{GOP}} \tag{3b}$$

$$\xi_W^{GOP}=\frac{2d_{GOP}}{t_{GOP}} \tag{3c}$$

$$\eta_W^{GOP}=\frac{\left(E_{GOP}/E_M\right)-1}{\left(E_{GOP}/E_M\right)+\xi_W^{GOP}} \tag{3d}$$

so that d_{GPL} and t_{GPL} define GOP average diameter and thickness, respectively. Furthermore, Poisson's ratio and density for GOP based composite might be defined based upon Poisson's ratio of the two constituents in the form

$$\begin{aligned}\nu_1&=\nu_{GOP}V_{GOP}+\nu_M V_M\\\rho_1&=\rho_{GOP}V_{GOP}+\rho_M V_M\end{aligned} \tag{4}$$

in which V_M=1−V_{GOP} expresses the volume fractions of matrix component. Herein, two dispersions of the GOP have been assumed as:

Uniform

$$V_{GOP}=V_{GOP}^{*} \tag{5}$$

Linear

$$V_{GOP}=(1+2\frac{z}{h})V_{GOP}^{*} \tag{6}$$

3. Refined plate theory

Based upon exact location of neutral surface when the material is graded, a refined four-unknown plate theory (Barati 2017, Fenjan *et al*. 2019, Ahmed *et al*. 2019, Abualnour *et al*. 2019, Addou *et al*. 2019, Balubaid *et al*. 2019, Batou *et al*. 2019, Draiche *et al*. 2019, Draoui *et al*. 2019, Hellal *et al*. 2019, Hussain *et al*. 2019, Mahmoudi *et al*. 2019, Medani *et al*. 2019, Meksi *et al*. 2019, Sahla *et al*. 2019, Semmah *et al*. 2019, Soltani *et al*. 2019, Tlidji *et al*. 2019, Tounsi *et al*. 2020, Zarga *et al*. 2019, Zaoui *et al*. 2019, Refrafi *et al*. 2020) presents a displacement field in

the below form

$$u_1(x,y,z,t)=u(x,y,t) -(z-z^*)\frac{\partial w_b}{\partial x}-[f(z)-z^{**}]\frac{\partial w_s}{\partial x} \tag{7}$$

$$u_2(x,y,z,t)=v(x,y,t) -(z-z^*)\frac{\partial w_b}{\partial y}-[f(z)-z^{**}]\frac{\partial w_s}{\partial y} \tag{8}$$

$$u_3(x,y,z,t)=w(x,y,t)=w_b(x,y,t)+w_s(x,y,t) \tag{9}$$

where

$$z^*=\frac{\int_{-h/2}^{h/2}E_1 z dz}{\int_{-h/2}^{h/2}E_1\,dz},\quad z^{**}=\frac{\int_{-h/2}^{h/2}E_1 f(z)dz}{\int_{-h/2}^{h/2}E_1\,dz} \tag{10}$$

Membrane displacement components have been respectively shown by u and v (Boukhlif *et al*. 2019). Furthermore, bending displacement components have been shown by w_b and w_s (Atmane *et al*. 2015, Draiche *et al*. 2019, Abdelaziz *et al*. 2017, Ayache *et al*. 2018, Bennai *et al*. 2019, Safa *et al*. 2019, Nebab *et al*. 2019). In order to incorporate shear deformations, the below function has been introduced

$$f(z)=z-\frac{h}{\pi}(\mathrm{Sin}[\frac{\pi z}{h}]) \tag{11}$$

Based on the proposed finite strip via refined plate theory, the governing equations might be represented by (Ahmed *et al*. 2019)

$$\frac{\partial N_x}{\partial x}+\frac{\partial N_{xy}}{\partial y}=I_0\frac{\partial^2 u}{\partial t^2}-I_1\frac{\partial^3 w_b}{\partial x\partial t^2}-I_3\frac{\partial^3 w_s}{\partial x\partial t^2} \tag{12}$$

$$\frac{\partial N_{xy}}{\partial x}+\frac{\partial N_y}{\partial y}=I_0\frac{\partial^2 v}{\partial t^2}-I_1\frac{\partial^3 w_b}{\partial y\partial t^2}-I_3\frac{\partial^3 w_s}{\partial y\partial t^2} \tag{13}$$

$$\begin{aligned}&\frac{\partial^2 M_x^b}{\partial x^2}+2\frac{\partial^2 M_{xy}^b}{\partial x\partial y}+\frac{\partial^2 M_y^b}{\partial y^2}-k_w w+\\ &+k_p(\frac{\partial^2(w_b+w_s)}{\partial x^2}+\frac{\partial^2(w_b+w_s)}{\partial y^2})=f(t)\\ &+I_0\frac{\partial^2(w_b+w_s)}{\partial t^2}+I_1(\frac{\partial^3 u}{\partial x\partial t^2}+\frac{\partial^3 v}{\partial y\partial t^2})\\ &-I_2\nabla^2(\frac{\partial^2 w_b}{\partial t^2})-I_4\nabla^2(\frac{\partial^2 w_s}{\partial t^2})\end{aligned} \tag{14}$$

$$\begin{aligned}&\frac{\partial^2 M_x^s}{\partial x^2}+2\frac{\partial^2 M_{xy}^s}{\partial x\partial y}+\frac{\partial^2 M_y^s}{\partial y^2}+\frac{\partial Q_{xz}}{\partial x}+\frac{\partial Q_{yz}}{\partial y}\\ &-k_w w+k_p(\frac{\partial^2(w_b+w_s)}{\partial x^2}+\frac{\partial^2(w_b+w_s)}{\partial y^2})=f(t)\\ &+I_0\frac{\partial^2(w_b+w_s)}{\partial t^2}+I_3(\frac{\partial^3 u}{\partial x\partial t^2}+\frac{\partial^3 v}{\partial y\partial t^2})\\ &-I_4\nabla^2(\frac{\partial^2 w_b}{\partial t^2})-I_5\nabla^2(\frac{\partial^2 w_s}{\partial t^2})\end{aligned} \tag{15}$$

so that $f(t)$ denotes the exerted impulse loading and

$$\begin{aligned}&(I_0,I_1,I_2,I_3,I_4,I_5)=\int_{-h/2}^{h/2}(1,z-z^*,(z-z^*)^2,\\ &f-z^{**},(z-z^*)(f-z^{**}),(f-z^{**})^2)\rho_1\,dz\end{aligned} \tag{16}$$

Also, N, M^b, M^s and Q denote in-plane axial force, bending moment, shearing moment and shear load which may be introduced by (Faleh *et al*. 2018, She *et al*. 2018)

$$\sigma_{ij}=C_{ijkl}\,\varepsilon_{kl} \tag{17}$$

where C_{ijkl} are elastic constants. Also, σ_{ij} and ε_{kl} denote the stress and strain field components. For a refined finite strip, the constitutive relations may be defined as

$$\begin{Bmatrix}\sigma_x\\ \sigma_y\\ \sigma_{xy}\\ \sigma_{yz}\\ \sigma_{xz}\end{Bmatrix}=\frac{E_1}{1-\nu_1^2}\begin{pmatrix}1 & \nu_1 & 0 & 0 & 0\\ \nu_1 & 1 & 0 & 0 & 0\\ 0 & 0 & (1-\nu_1)/2 & 0 & 0\\ 0 & 0 & 0 & (1-\nu_1)/2 & 0\\ 0 & 0 & 0 & 0 & (1-\nu_1)/2\end{pmatrix}\begin{Bmatrix}\varepsilon_x\\ \varepsilon_y\\ \gamma_{xy}\\ \gamma_{yz}\\ \gamma_{xz}\end{Bmatrix} \tag{18}$$

Integration from above system of equations in thickness direction gives the below resultants

$$\begin{Bmatrix}N_x\\ N_y\\ N_{xy}\end{Bmatrix}=A\begin{pmatrix}1 & \nu & 0\\ \nu & 1 & 0\\ 0 & 0 & (1-\nu)/2\end{pmatrix}\begin{Bmatrix}\frac{\partial u}{\partial x}\\ \frac{\partial v}{\partial y}\\ \frac{\partial u}{\partial y}+\frac{\partial v}{\partial x}\end{Bmatrix} \tag{19}$$

$$\begin{aligned}&\begin{Bmatrix}M_x^b\\ M_y^b\\ M_{xy}^b\end{Bmatrix}=D\begin{pmatrix}1 & \nu & 0\\ \nu & 1 & 0\\ 0 & 0 & (1-\nu)/2\end{pmatrix}\begin{Bmatrix}-\frac{\partial^2 w_b}{\partial x^2}\\ -\frac{\partial^2 w_b}{\partial y^2}\\ -2\frac{\partial^2 w_b}{\partial x\partial y}\end{Bmatrix}\\ &+E\begin{pmatrix}1 & \nu & 0\\ \nu & 1 & 0\\ 0 & 0 & (1-\nu)/2\end{pmatrix}\begin{Bmatrix}-\frac{\partial^2 w_s}{\partial x^2}\\ -\frac{\partial^2 w_s}{\partial y^2}\\ -2\frac{\partial^2 w_s}{\partial x\partial y}\end{Bmatrix}\end{aligned} \tag{20}$$

$$\begin{Bmatrix}M_x^s\\ M_y^s\\ M_{xy}^s\end{Bmatrix}=E\begin{pmatrix}1 & \nu & 0\\ \nu & 1 & 0\\ 0 & 0 & (1-\nu)/2\end{pmatrix}\begin{Bmatrix}-\frac{\partial^2 w_b}{\partial x^2}\\ -\frac{\partial^2 w_b}{\partial y^2}\\ -2\frac{\partial^2 w_b}{\partial x\partial y}\end{Bmatrix}$$

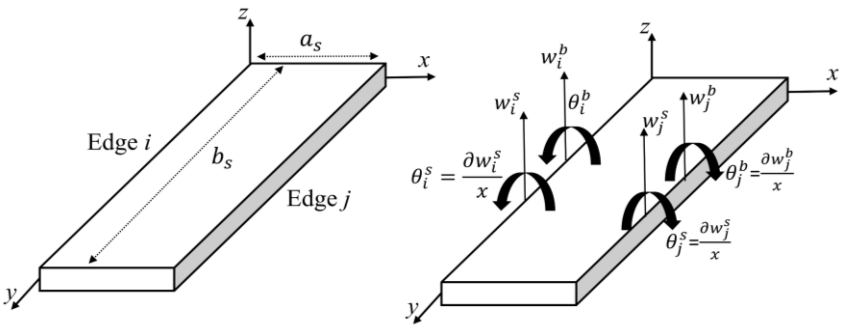

Fig. 2 Refined finite strip and nodal coordinates

$$+F\begin{pmatrix}1 & \nu & 0\\ \nu & 1 & 0\\ 0 & 0 & (1-\nu)/2\end{pmatrix}\begin{Bmatrix}-\frac{\partial^2 w_S}{\partial x^2}\\ -\frac{\partial^2 w_S}{\partial y^2}\\ -2\frac{\partial^2 w_S}{\partial x\partial y}\end{Bmatrix} \tag{21}$$

$$\begin{Bmatrix}Q_x\\ Q_y\end{Bmatrix} = A_{44}\begin{pmatrix}1 & 0\\ 0 & 1\end{pmatrix}\begin{Bmatrix}\frac{\partial w_S}{\partial x}\\ \frac{\partial w_S}{\partial y}\end{Bmatrix} \tag{22}$$

in which:

$$A=\int_{-h/2}^{h/2}\frac{E_1}{1-\nu_1^2}dz,\quad D=\int_{-h/2}^{h/2}\frac{E_1(z-z^*)^2}{1-\nu_1^2}dz,$$
$$R=\int_{-h/2}^{h/2}\frac{E_1(z-z^*)(f-z^{**})}{1-\nu_1^2}dz \tag{23}$$
$$F=\int_{-h/2}^{h/2}\frac{E_1(f-z^{**})^2}{1-\nu_1^2}dz,\quad A_{44}=\int_{-h/2}^{h/2}\frac{E_1}{2(1+\nu_1)}g^2dz$$

where g=1-df/dz. Note that I_1 and I_3 in Eq. (16) are zero due to considering exact position of neutral surface. Therefore, the coupling between Eqs. (12)-(13) and Eqs. (14)-(15) has been eliminated. Now, one can get to the governing equations of the GOP-reinforced plate by inserting Eqs. (19)-(22), into Eqs. (14)-(15) as follows

$$\begin{aligned}&-D(\frac{\partial^4 w_b}{\partial x^4}+2\frac{\partial^4 w_b}{\partial x^2\partial y^2}+\frac{\partial^4 w_b}{\partial y^4})\\ &-R(\frac{\partial^4 w_s}{\partial x^4}+2\frac{\partial^4 w_s}{\partial x^2\partial y^2}+\frac{\partial^4 w_s}{\partial y^4})\\ &+(-I_0\frac{\partial^2(w_b+w_s)}{\partial t^2}+I_2(\frac{\partial^2}{\partial x^2}+\frac{\partial^2}{\partial y^2})(\frac{\partial^2 w_b}{\partial t^2})\\ &+I_4(\frac{\partial^2}{\partial x^2}+\frac{\partial^2}{\partial y^2})(\frac{\partial^2 w_s}{\partial t^2})=f(t)\end{aligned} \tag{24}$$

$$\begin{aligned}&-R(\frac{\partial^4 w_b}{\partial x^4}+2\frac{\partial^4 w_b}{\partial x^2\partial y^2}+\frac{\partial^4 w_b}{\partial y^4})-F(\frac{\partial^4 w_s}{\partial x^4}\\ &+2\frac{\partial^4 w_s}{\partial x^2\partial y^2}+\frac{\partial^4 w_s}{\partial y^4})+A_{44}(\frac{\partial^2 w_s}{\partial x^2}+\frac{\partial^2 w_s}{\partial y^2})\\ &+(-I_0\frac{\partial^2(w_b+w_s)}{\partial t^2}+I_4(\frac{\partial^2}{\partial x^2}+\frac{\partial^2}{\partial y^2})(\frac{\partial^2 w_b}{\partial t^2})\\ &+I_5(\frac{\partial^2}{\partial x^2}+\frac{\partial^2}{\partial y^2})(\frac{\partial^2 w_s}{\partial t^2}))=f(t)\end{aligned} \tag{25}$$

The impulse loading is defined as a point load in the following form where f_0 denotes load amplitude and (x_0, y_0) is load location:

Sinusoidal pulse load

$$f(t)=f_0\sin\left(\frac{\pi t}{t_0}\right)\delta(x-x_0)\\ \delta(y-y_0)[H(t)-H(t-t_0)] \tag{26}$$

Linear pulse load

$$f(t)=f_0\delta(x-x_0)\delta(y-y_0)\\ \left(1-\frac{t}{t_0}\right)(H(t)-H(t-t_0)) \tag{27}$$

Blast load

$$f(t)=1.8\,f_0\delta(x-x_0)\delta(y-y_0)\\ \left(1-\frac{t}{t_0}\right)e^{\left(\frac{-r_b t}{t_0}\right)}(H(t)-H(t-t_0)) \tag{28}$$

where r_b is a factor representing the decaying rate of the pulse load.

4. Finite strip method (FSM)

In this section, the finite strip method (Cheung 1968) based upon proposed refined plate model, which is known as refined finite strip method, has been used for investigating the transient vibrational behavior of GOP-reinforced plate. Fig. 2 illustrates a single strip having length a_s and width b_s with two nodal lines of i and j. This figure also shows the strip nodal degrees of freedom. As the first step, the bending and shear displacements of the strip can be introduced by

$$w_b=\sum_{e=1}^{r}f_e^{w_b}(x)g_e^{w_b}(y) \tag{29}$$

$$w_s=\sum_{e=1}^{r}f_e^{w_s}(x)g_e^{w_s}(y) \tag{30}$$

where r defines the number of harmonic modes, $f_e^{w_b}(x)$

and $f_e^{w_s}(x)$ are appropriate Hermitian shape functions; $g_e^{w_b}(y)$ and $g_e^{w_s}(y)$ are trigonometric functions satisfying boundary conditions at *y* direction.

Based on Hermitian shape functions, Eqs. (29) and (30) can be re-written as

$$w_b = \sum_{e=1}^{r} \begin{bmatrix} (1-3\zeta^2+2\zeta^3)(w_i^b)_e \\ +(3\zeta^2-2\zeta^3)(w_j^b)_e + \\ +a_s(\zeta-2\zeta^2+\zeta^3)(\theta_i^b)_e \\ a_s(-\zeta^2+\zeta^3)(\theta_j^b)_e \end{bmatrix} g_e^{w_b}(y) \tag{31}$$

$$w_s = \sum_{e=1}^{r} \begin{bmatrix} (1-3\zeta^2+2\zeta^3)(w_i^s)_e \\ +(3\zeta^2-2\zeta^3)(w_j^s)_e + \\ +a_s(\zeta-2\zeta^2+\zeta^3)(\theta_i^s)_e \\ a_s(-\zeta^2+\zeta^3)(\theta_j^s)_e \end{bmatrix} g_e^{w_s}(y) \tag{32}$$

in which $\zeta=x/a_s$ and $\{w_i^b \ \theta_i^b \ w_j^b \ \theta_j^b\}$ are bending degrees of freedom of each nodal line, whereas $\{w_i^s \ \theta_i^s \ w_j^s \ \theta_j^s\}$ are the shear degrees of freedom. Eqs. (31) and (32) can then be re-written in vector forms as (Huang and Thambiratnam 2001)

$$w_b = \sum_{e=1}^{r} N_e^b \delta_e^b \tag{33}$$

$$w_s = \sum_{e=1}^{r} N_e^s \delta_e^s \tag{34}$$

where

$$N_e^b = N_e^s = [1-3\zeta^2+2\zeta^3 \quad a_s(\zeta-2\zeta^2+\zeta^3) \quad 3\zeta^2-2\zeta^3 \quad a_s(-\zeta^2+\zeta^3)]g_e^{w_b}(y) \tag{35}$$

Also, δ_e^b and δ_e^s are the displacement vectors related to mode *e* and has the following form

$$\delta_e^b = \{w_i^b \ \theta_i^b \ w_j^b \ \theta_j^b\}_e^T = \begin{Bmatrix} (\delta_i^b)_e \\ (\delta_j^b)_e \end{Bmatrix} \tag{36}$$

$$\delta_e^s = \{w_i^s \ \theta_i^s \ w_j^s \ \theta_j^s\}_e^T = \begin{Bmatrix} (\delta_i^s)_e \\ (\delta_j^s)_e \end{Bmatrix} \tag{37}$$

Then, the complete displacement vector for a strip can be represented as

$$\delta = \{w_i^b \ \theta_i^b \ w_j^b \ \theta_j^b \ w_i^s \ \theta_i^s \ w_j^s \ \theta_j^s\}_e^T = \begin{Bmatrix} \delta_i^b \\ \delta_j^b \\ \delta_i^s \\ \delta_j^s \end{Bmatrix} \tag{38}$$

Using the weak form of the governing equation and constructing Hamiltonian (*H*) and minimizing it to field coefficients (Rezaiee-Pajand *et al*. 2018, Al-Maliki *et al*. 2019) results in below relation containing simultaneous algebraic equations

$$\frac{\partial H}{\partial \delta} = 0 \tag{39}$$

Introducing Eqs. (33)-(34) to obtained relations yields

$$[K]\{\delta\}+[M]\{\ddot{\delta}\} = \{F(t)\} \tag{40}$$

Utilizing Laplace transform approach in Eq. (40) together with the consideration of zero initial conditions, the below system of equation would be derived

$$[K]\{L[\delta]\}+[M]\{L[\delta]\} = \{L[F(t)]\} \tag{41}$$

where is *S* is Laplace transform operator. The following boundary conditions for the edge strips can be considered:

Simply supported edge (S)

$$w_b = w_s = 0, \quad \frac{\partial^2 w_b}{\partial x^2} = \frac{\partial^2 w_s}{\partial x^2} = \frac{\partial^2 w_b}{\partial y^2} = \frac{\partial^2 w_s}{\partial y^2} = 0 \tag{42}$$

Clamped edge (C):

$$w_b = w_s = 0, \quad \frac{\partial w_b}{\partial x} = \frac{\partial w_s}{\partial x} = \frac{\partial w_b}{\partial y} = \frac{\partial w_s}{\partial y} = 0 \tag{43}$$

Via solving Eq. (41) and utilizing inverse Laplace transform approach, it is feasible to derive total maximum deflection of the plate at its center (*W*). In order to represent the obtained results, the below dimensionless parameters may be introduced

$$t^* = \frac{t}{t_0}, \bar{W} = W\frac{E_{GOP}I}{f_0 a^3}, K_w = \frac{k_w a^4}{D_G}, \quad K_P = \frac{k_P a^2}{D_G}, D_G = \frac{E_{GOP}h^3}{12(1-\nu_{GOP}^2)} \tag{44}$$

5. Numerical results and discussions

Based on refined plate strip, the problem of transient vibration of GOP-reinforced plates was formulated and solved in previous sections. Now, this section provides new results for considered problem to show the importance of several factors including GOP distribution, exerted pulse loads, load position, load duration, foundation parameters and boundary condition on transient response of the plate. Fig. 1 illustrates a GOP-reinforced plate on elastic foundation and subjected to three types of pulse load which their variation against time is illustrated in Fig. 3.

Also, vibration frequencies for nano-composite plates reinforced by carbon nanotubes (CNTs) are validated with those reported by Zhu *et al*. (2012) and the results are presented as Table 1. Different number of strips have been

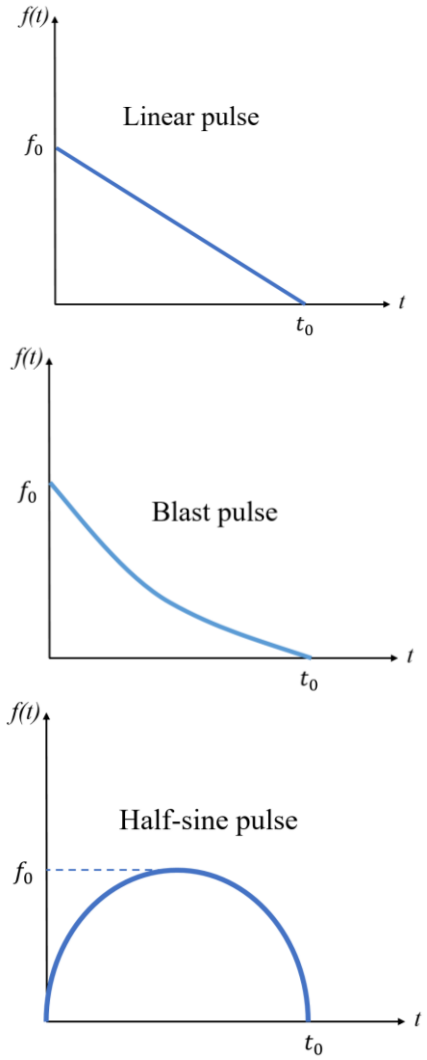

Fig. 3 Variations different pulse loads with respect to the time

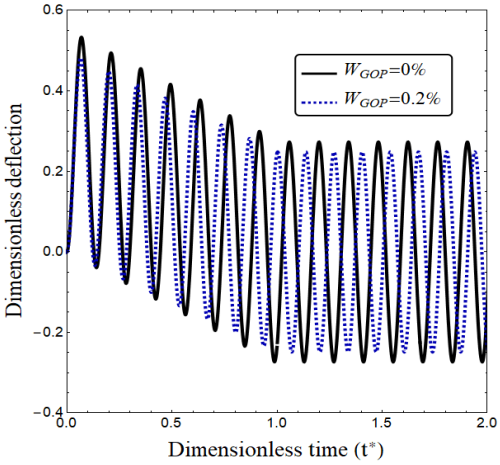

(a) Linear pulse load

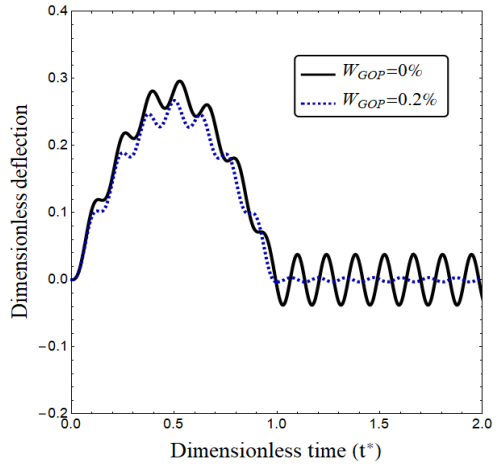

(b) Half-sine pulse load

Fig. 4 Dynamic response of the plate for different GOP weight fraction and exerted impulse loadings (a/h=10, t_0=0.03)

Table 1 Validation of dimensionless frequency for nano-composite plates

	Present FSM solution				
	2 strips	3 strips	5 strips	8 strips	Zhu *et al.* (2012)
V_{cnt}=0.11	14.137	13.742	13.581	13.533	13.532
V_{cnt}=0.14	14.891	14.465	14.393	14.306	14.306
V_{cnt}=0.17	17.613	17.224	16.926	16.816	16.815

considered for validation study. Considering 8 strips, obtained frequencies based on various values of CNT volume fraction (V_{cnt}) are in excellent agreement with those of Zhu *et al.* (2012). New results related to transient vibration of GOP-reinforced plates have been presented and explained in the following paragraphs. In the present study, the material properties of GOP reinforced plate with concrete matrix are considered as:

- $E_{GOP} = 444.8\,TPa$, $d_{GOP} = 500\,nm$, $t_{GOP} = 0.95\,nm$, $v_{GOP} = 0.165$.
- $E_M = 16.9\,TPa$, $v_M = 0.15$.

In Fig. 4 the time response of GOP-reinforced plate due to exerted linear and sinusoidal pulse loads is illustrated for various values of GOP weight fraction by assuming that loading time is t_0=0.05 s. Uniform GOP distribution has been considered. First, it should be pointed out that when the dimensionless time (t*) varies from 0 to 1, the GOP-reinforced plate experiences transient vibrations due to pulse loads. After t*=1, free vibrations of the plate can be seen. However, by increasing in t* for the case of linear impulse load the transient vibrations linearly (not suddenly) reach to the free oscillations. Also, reinforcing effect of GOPs on dynamic behavior of the plate is clearly observable in this figure. Actually, the effective stiffness of the reinforced plate can be greatly strengthened by dispersing a small amount of GOPs into matrix material. Accordingly, by increase of GOP weight fraction, the dynamic deflections will reduce.

In Fig. 5, transient vibration response of GOP-reinforced plate under linear pulse load has been presented accounting for various GOP weight fraction and dispersions. It is considered that a/h=10 and t_0=0.03. The most important observation from this figure is that increasing GOP weight fraction yields lower dynamic deflection for all types of GOP distributions. It means that adding the amount of GOP can increase the plate stiffness and enhance its vibration

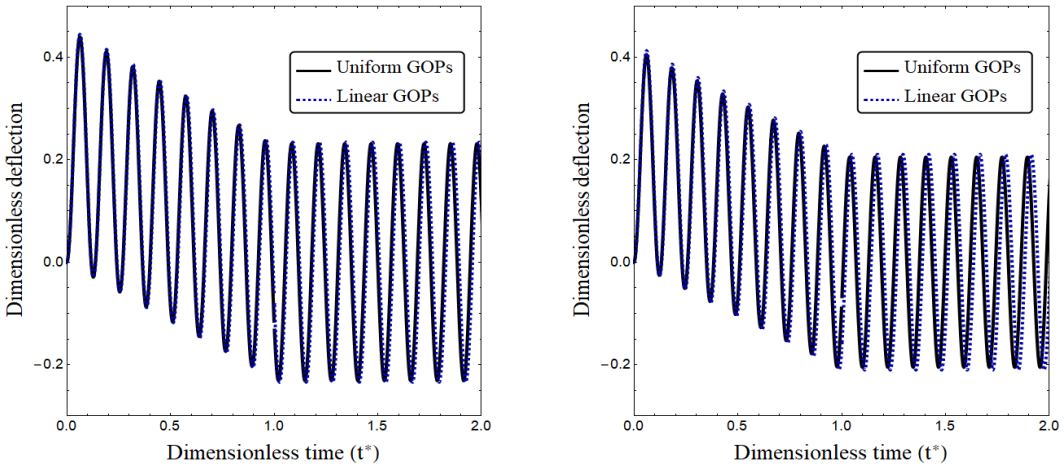

(a) W_{GOP}=0.4% (b) W_{GOP}=0.6%

Fig. 5 Dynamic response of the plate for different GOP distributions (a/h=10, t_0=0.05)

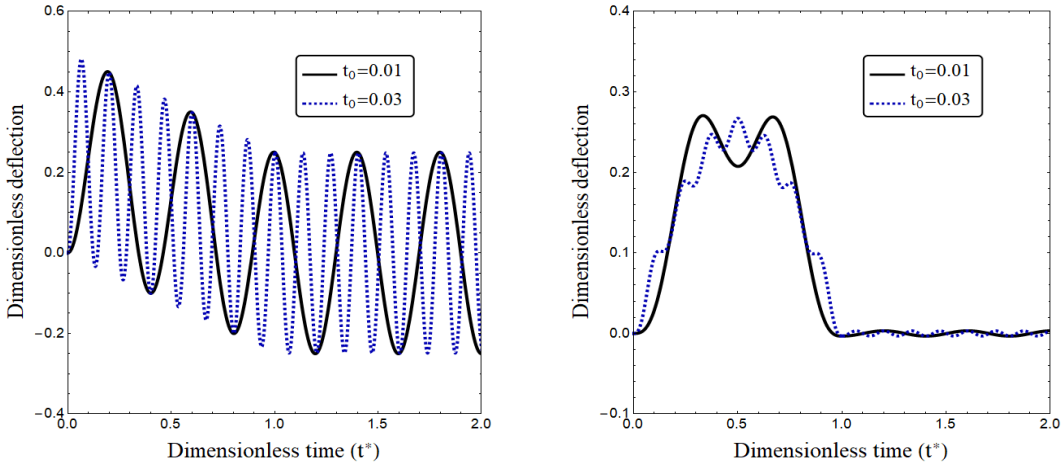

(a) Linear pulse load (b) Half-Sine pulse load

Fig. 6 Dynamic response of the plate for different loading time (W_{GOP}=0.2%, a/h=10)

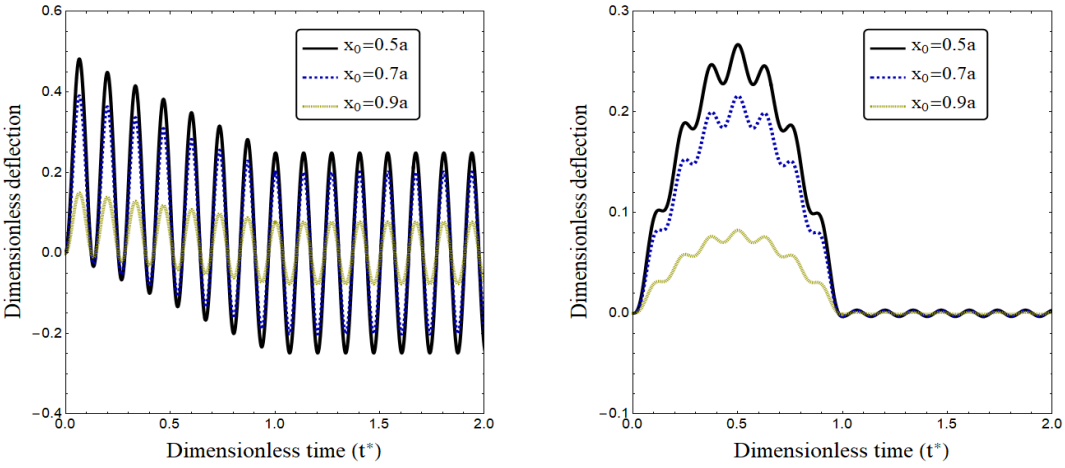

(a) Linear pulse load (b) Half-Sine pulse load

Fig. 7 Dynamic response of the plate for different load positions (W_{GOP}=0.2%, a/h=10)

character. Moreover, uniform GOP distribution provides smaller dynamic deflection than linear distribution. This is due to higher volume of GOP within the nano-composite plate.

Impacts of loading time (t_0) on dynamic characteristics of a GOP-reinforced plate under pulse loads has been studied in Fig. 6. It is evident that the number of oscillations in transient zone becomes greater as the amount of loading

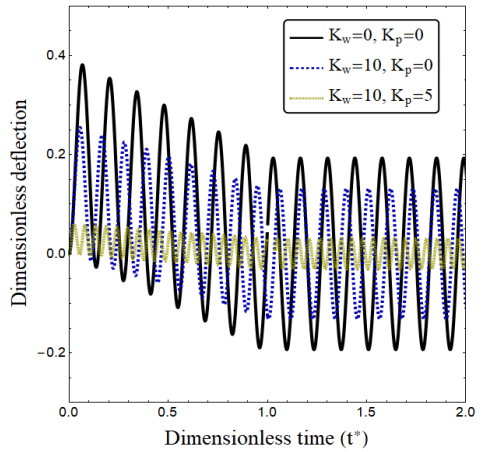

Fig. 8 Dynamic response of the plate for different foundation parameters (W_{GOP}=0.2%, a/h=10)

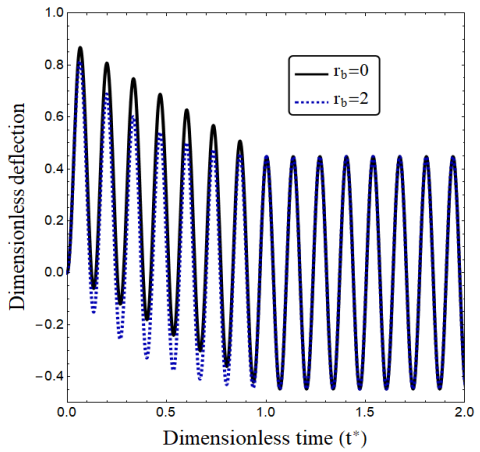

Fig. 10 Dynamic response of the plate for different blast load parameters (W_{GOP}=0.2%, a/h=10)

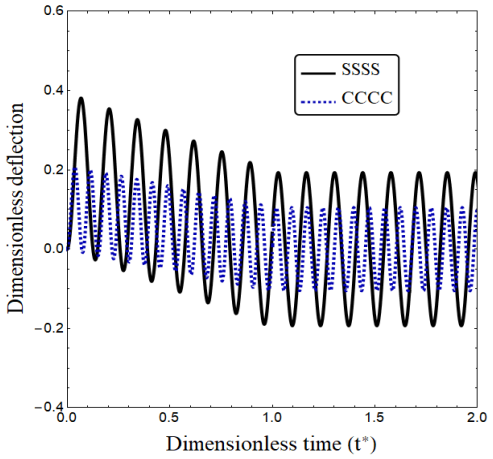

(a) Linear pulse load

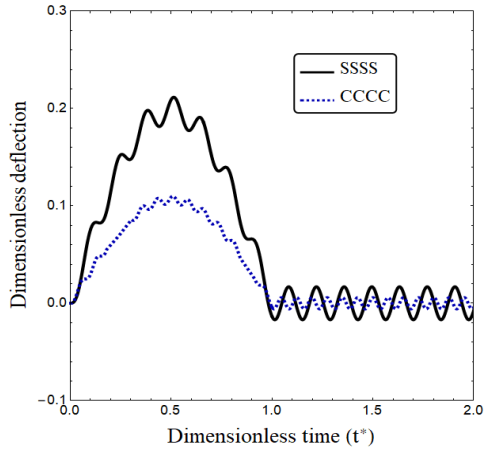

(b) Half-sine pulse load

Fig. 9 Dynamic response of the plate for different boundary conditions (a/h=10, W_{GOP}=0.2%)

time becomes larger. However, loading time have great influence on dimensionless deflection in transient region. As a conclusion, one can state that as the loading time is smaller the plate passes from the transient region with fewer number of oscillations.

Fig. 7 shows the influence of loading location on dynamic characteristics of a GOP-reinforced plate under pulse loads when t_0=0.03. It can be concluded from the figure that as the loading point travels far from the center of GOP-reinforced plate, the dynamical deflection in transient zone becomes smaller. So, the maximum deflection occurs when the pulse load is placed at the center point of GOP-reinforced plate. Also, load location has no effect on number of oscillations in the transient region.

Fig. 8 indicates the dimensionless deflection of a GOP-reinforced plate versus dimensionless amplitude for various linear (K_W) and shear (K_P) foundation parameters at W_{GOP}=0.2%. It should be mentioned that the shear layer provides a continuous interaction with the GOP-reinforced plate, while linear layer has a discontinuous interaction with the plate. Increasing foundation parameters yields smaller dynamic deflections by enhancing the bending rigidity of the GOP-reinforced plate. So the GOP-reinforced plate rested on elastic foundation experiences transient vibrations with lower deflections.

Effect of boundary condition on transient vibration characteristics of a GOP-reinforced plate under pulse loads has been plotted in Fig. 9. Both fully clamped and fully simply-supported boundary conditions have been considered. Obtained results show that a considerable reduction in dynamic deflection of the plate occurs by applying clamped conditions. This means that clamped edges makes the structure stiffer leading to transient vibrations of the plate with lower magnitude of deflection.

Time response of the plate under blast load based on various blast load parameter (r_b) has been illustrated in Fig. 10. It is considered that a/h=10 and t_0=0.03. It can be seen that blast load parameter has a great influence on transient vibration of the GOP-reinforced plate. Actually, this parameter determines the rate of passing from transient to free vibrations. So, as the blast load parameter increases, the dynamic deflections of the plate become larger and transient vibration become closer to the free vibration region with a higher rate.

6. Conclusions

Based on finite strip method (FSM), the present article

was devoted to investigate transient characteristics of a higher-order shear deformable GOP-reinforced plate exposed to different kinds of impulsive loads. GOP dispersion was considered to be uniform or linear inside the matrix. Three impulse loads of sinusoidal-type, linear-type and blast-type were applied. The governing equations were solved employing FSM and inverse Laplace transform technique. Actually, the effective stiffness of the reinforced plate can be greatly strengthened by dispersing a small amount of GOPs into matrix material. Thus, dynamic deflection decreases with the increase of GOP weight fraction. Moreover, uniform GOP distribution provides smaller dynamic deflection than linear distribution. Also, it was found that as the loading time is smaller the plate passes from the transient region with fewer number of oscillations. Moreover, as the blast load parameter increases, the dynamic deflections become larger and transient vibration become closer to the free vibration region with higher slope.

Acknowledgement

The first and second authors would like to thank FPQ (Fidar project Qaem) for providing the fruitful and useful help.

References

Abdelaziz, H.H., Meziane, M.A.A., Bousahla, A.A., Tounsi, A., Mahmoud, S.R. and Alwabli, A.S. (2017), "An efficient hyperbolic shear deformation theory for bending, buckling and free vibration of FGM sandwich plates with various boundary conditions", *Steel Compos. Struct.*, **25**(6), 693-704. https://doi.org/10.12989/scs.2017.25.6.693.

Abualnour, M., Chikh, A., Hebali, H., Kaci, A., Tounsi, A., Bousahla, A.A. and Tounsi, A. (2019), "Thermomechanical analysis of antisymmetric laminated reinforced composite plates using a new four variable trigonometric refined plate theory", *Comput. Concrete*, **24**(6), 489-498. https://doi.org/10.12989/cac.2019.24.6.489.

Addou, F.Y., Meradjah, M., Bousahla, A.A., Benachour, A., Bourada, F., Tounsi, A. and Mahmoud, S.R. (2019), "Influences of porosity on dynamic response of FG plates resting on Winkler/Pasternak/Kerr foundation using quasi 3D HSDT", *Comput. Concrete*, **24**(4), 347-367. https://doi.org/10.12989/cac.2019.24.4.347.

Ahankari, S.S and Kar, K.K. (2010), "Hysteresis measurements and dynamic mechanical characterization of functionally graded natural rubber–carbon black composites", *Polym. Eng. Sci.*, **50**(5), 871-877. https://doi.org/10.1002/pen.21601.

Ahmed, R.A., Fenjan, R.M. and Faleh, N.M. (2019), "Analyzing post-buckling behavior of continuously graded FG nanobeams with geometrical imperfections", *Geomech. Eng.*, **17**(2), 175-180. https://doi.org/10.12989/gae.2019.17.2.175.

Al-Maliki, A.F., Faleh, N.M. and Alasadi, A.A. (2019), "Finite element formulation and vibration of nonlocal refined metal foam beams with symmetric and non-symmetric porosities", *Struct. Monit. Mainten.*, **6**(2), 147-159. https://doi.org/10.12989/smm.2019.6.2.147.

Atmane, H.A., Tounsi, A., Bernard, F. and Mahmoud, S.R. (2015), "A computational shear displacement model for vibrational analysis of functionally graded beams with porosities", *Steel Compos. Struct.*, **19**(2), 369-384. https://doi.org/10.12989/scs.2015.19.2.369.

Ayache, B., Bennai, R., Fahsi, B., Fourn, H., Atmane, H.A. and Tounsi, A. (2018), "Analysis of wave propagation and free vibration of functionally graded porous material beam with a novel four variable refined theory", *Earthq. Struct.*, **15**(4), 369-382. https://doi.org/10.12989/eas.2018.15.4.369.

Azimi, M., Mirjavadi, S.S., Shafiei, N. and Hamouda, A.M.S. (2017), "Thermo-mechanical vibration of rotating axially functionally graded nonlocal Timoshenko beam", *Appl. Phys. A*, **123**(1), 104. https://doi.org/10.1007/s00339-016-0712-5.

Azimi, M., Mirjavadi, S.S., Shafiei, N., Hamouda, A.M.S. and Davari, E. (2018), "Vibration of rotating functionally graded Timoshenko nano-beams with nonlinear thermal distribution", *Mech. Adv. Mater. Struct.*, **25**(6), 467-480. https://doi.org/10.1080/15376494.2017.1285455.

Balubaid, M., Tounsi, A., Dakhel, B. and Mahmoud, S.R. (2019), "Free vibration investigation of FG nanoscale plate using nonlocal two variables integral refined plate theory. *Comput. Concrete*, **24**(6), 579-586. https://doi.org/10.12989/cac.2019.24.6.579.

Barati, M. R. (2017), "Nonlocal-strain gradient forced vibration analysis of metal foam nanoplates with uniform and graded porosities", *Adv. Nano Res.*, **5**(4), 393-414. https://doi.org/10.12989/anr.2017.5.4.393.

Barati, M.R. and Zenkour, A.M. (2018), "Analysis of postbuckling of graded porous GPL-reinforced beams with geometrical imperfection", *Mech. Adv. Mater. Struct.*, **26**(6), 503-511. https://doi.org/10.1080/15376494.2017.1400622.

Batou, B., Nebab, M., Bennai, R., Atmane, H. A., Tounsi, A. and Bouremana, M. (2019), "Wave dispersion properties in imperfect sigmoid plates using various HSDTs", *Steel Compos. Struct.*, **33**(5), 699. https://doi.org/10.12989/scs.2019.33.5.699.

Cheung, Y.K. (1968), "The finite strip method in the analys of elastic plates with two opposite simply supported ends", *Proc. Inst. Civil Eng.*, **40**(1), 1-7. https://doi.org/10.1680/iicep.1968.7709.

Draiche, K., Bousahla, A.A., Tounsi, A., Alwabli, A.S., Tounsi, A. and Mahmoud, S.R. (2019), "Static analysis of laminated reinforced composite plates using a simple first-order shear deformation theory", *Comput. Concrete*, **24**(4), 369-378. https://doi.org/10.12989/cac.2019.24.4.369.

Draoui, A., Zidour, M., Tounsi, A. and Adim, B. (2019), "Static and dynamic behavior of nanotubes-reinforced sandwich plates using (FSDT)", *J. Nano Res.*, **57**, 117-135. https://doi.org/10.4028/www.scientific.net/JNanoR.57.117.

Du, H., Gao, H.J. and Dai Pang, S. (2016), "Improvement in concrete resistance against water and chloride ingress by adding graphene nanoplatelet", *Cement Concrete Res.*, **83**, 114-123. https://doi.org/10.1016/j.cemconres.2016.02.005.

Esawi, A.M.K., Morsi, K., Sayed, A., Taher, M. and Lanka, S. (2011), "The influence of carbon nanotube (CNT) morphology and diameter on the processing and properties of CNT-reinforced aluminium composites", *Compos. Part A: Appl. Sci. Manuf.*, **42**(3), 234-243. https://doi.org/10.1016/j.compositesa.2010.11.008.

Faleh, N.M., Ahmed, R.A. and Fenjan, R.M. (2018), "On vibrations of porous FG nanoshells", *Int. J. Eng. Sci*., **133**, 1-14. https://doi.org/10.1016/j.ijengsci.2018.08.007.

Fang, M., Wang, K., Lu, H., Yang, Y. and Nutt, S. (2009). Covalent polymer functionalization of graphene nanosheets and mechanical properties of composites", *J. Mater. Chem.*, **19**(38), 7098-7105. https://doi.org/10.1039/B908220D.

Feng, C., Kitipornchai, S. and Yang, J. (2017). Nonlinear free vibration of functionally graded polymer composite beams reinforced with graphene nanoplatelets (GPLs)", *Eng. Struct.*, **140**, 110-119. https://doi.org/10.1016/j.engstruct.2017.02.052.

Fenjan, R.M., Ahmed, R.A., Alasadi, A.A. and Faleh, N.M.

(2019), "Nonlocal strain gradient thermal vibration analysis of double-coupled metal foam plate system with uniform and non-uniform porosities", *Coupl. Syst. Mech.*, **8**(3), 247-257. https://doi.org/10.12989/csm.2019.8.3.247.

Gojny, F.H., Wichmann, M.H.G., Köpke, U., Fiedler, B and Schulte, K. (2004), "Carbon nanotube-reinforced epoxy-composites: enhanced stiffness and fracture toughness at low nanotube content", *Compos. Sci. Technol.*, **64**(15), 2363-2371. https://doi.org/10.1016/j.compscitech.2004.04.002.

Hellal, H., Bourada, M., Hebali, H., Bourada, F., Tounsi, A., Bousahla, A.A. and Mahmoud, S.R. (2019). Dynamic and stability analysis of functionally graded material sandwich plates in hygro-thermal environment using a simple higher shear deformation theory", *J. Sandw. Struct. Mater.*, 1099636219845841. https://doi.org/10.1177%2F1099636219845841.

Huang, M.H. and Thambiratnam, D.P. (2001), "Analysis of plate resting on elastic supports and elastic foundation by finite strip method", *Comput. Struct.*, **79**(29-30), 2547-2557. https://doi.org/10.1016/S0045-7949(01)00134-1.

Hussain, M., Naeem, M.N., Tounsi, A. and Taj, M. (2019), "Nonlocal effect on the vibration of armchair and zigzag SWCNTs with bending rigidity", *Adv. Nano Res.*, **7**(6), 431. https://doi.org/10.12989/anr.2019.7.6.431.

Keleshteri, M.M., Asadi, H. and Wang, Q. (2017). Large amplitude vibration of FG-CNT reinforced composite annular plates with integrated piezoelectric layers on elastic foundation", *Thin Wall. Struct.*, **120**, 203-214. https://doi.org/10.1016/j.tws.2017.08.035.

King, J.A., Klimek, D.R., Miskioglu, I. and Odegard, G. M. (2013). Mechanical properties of graphene nanoplatelet/epoxy composites", *J. Appl. Polym. Sci.*, **128**(6), 4217-4223. https://doi.org/10.1002/app.38645.

Kitipornchai, S., Chen, D. and Yang, J. (2017). Free vibration and elastic buckling of functionally graded porous beams reinforced by graphene platelets", *Mater. Des.*, **116**, 656-665. https://doi.org/10.1016/j.matdes.2016.12.061.

Lal, A. and Markad, K. (2018), "Deflection and stress behaviour of multi-walled carbon nanotube reinforced laminated composite beams", *Comput. Concrete*, **22**(6), 501-514. https://doi.org/10.12989/cac.2018.22.6.501.

Liew, K.M., Lei, Z.X. and Zhang, L.W. (2015). Mechanical analysis of functionally graded carbon nanotube reinforced composites: a review", *Compos. Struct.*, **120**, 90-97. https://doi.org/10.1016/j.compstruct.2014.09.041.

Lin, F., Yang, C., Zeng, Q.H and Xiang, Y. (2018), "Morphological and mechanical properties of graphene-reinforced PMMA nanocomposites using a multiscale analysis", *Compu. Mater. Sci.*, **150**, 107-120. https://doi.org/10.1016/j.commatsci.2018.03.048.

Mahmoudi, A., Benyoucef, S., Tounsi, A., Benachour, A., Adda Bedia, E.A. and Mahmoud, S.R. (2019), "A refined quasi-3D shear deformation theory for thermo-mechanical behavior of functionally graded sandwich plates on elastic foundations", *J. Sandw. Struct. Mater.*, **21**(6), 1906-1929. https://doi.org/10.1177%2F1099636217727577.

Medani, M., Benahmed, A., Zidour, M., Heireche, H., Tounsi, A., Bousahla, A.A. and Mahmoud, S.R. (2019), "Static and dynamic behavior of (FG-CNT) reinforced porous sandwich plate using energy principle", *Steel Compos. Struct.*, **32**(5), 595-610. https://doi.org/10.12989/scs.2019.32.5.595.

Meksi, R., Benyoucef, S., Mahmoudi, A., Tounsi, A., Adda Bedia, E. A. and Mahmoud, S. R. (2019), "An analytical solution for bending, buckling and vibration responses of FGM sandwich plates", *J. Sandw. Struct. Mater.*, **21**(2), 727-757. https://doi.org/10.1177%2F1099636217698443.

Mirjavadi, S.S., Afshari, B.M., Barati, M.R. and Hamouda, A.M.S. (2018), "Strain gradient based dynamic response analysis of heterogeneous cylindrical microshells with porosities under a moving load", *Mater. Res. Exp.*, **6**(3), 035029.

Mirjavadi, S.S., Afshari, B.M., Barati, M.R. and Hamouda, A.M.S. (2019), "Transient response of porous FG nanoplates subjected to various pulse loads based on nonlocal stress-strain gradient theory", *Eur. J. Mech.-A/Solid.*, **74**, 210-220. https://doi.org/10.1016/j.euromechsol.2018.11.004.

Mirjavadi, S.S., Afshari, B.M., Barati, M.R. and Hamouda, A.M.S. (2019), "Nonlinear free and forced vibrations of graphene nanoplatelet reinforced microbeams with geometrical imperfection", *Microsyst. Technol.*, **25**, 3137-3150. https://doi.org/10.1007/s00542-018-4277-4.

Mirjavadi, S.S., Afshari, B.M., Khezel, M., Shafiei, N., Rabby, S. and Kordnejad, M. (2018), "Nonlinear vibration and buckling of functionally graded porous nanoscaled beams", *J. Brazil. Soc. Mech. Sci. Eng.*, **40**(7), 352. https://doi.org/10.1007/s40430-018-1272-8.

Mirjavadi, S.S., Afshari, B.M., Shafiei, N., Hamouda, A.M.S. and Kazemi, M. (2017), "Thermal vibration of two-dimensional functionally graded (2D-FG) porous Timoshenko nanobeams", *Steel Compos. Struct.*, **25**(4), 415-426. https://doi.org/10.12989/scs.2017.25.4.415.

Mirjavadi, S.S., Forsat, M., Barati, M.R., Abdella, G.M., Afshari, B.M., Hamouda, A.M.S. and Rabby, S. (2019), "Dynamic response of metal foam FG porous cylindrical micro-shells due to moving loads with strain gradient size-dependency", *Eur. Phys. J. Plus*, **134**(5), 214. https://doi.org/10.1140/epjp/i2019-12540-3.

Mirjavadi, S.S., Forsat, M., Barati, M.R., Abdella, G.M., Hamouda, A.M.S., Afshari, B.M. and Rabby, S. (2019), "Post-buckling analysis of piezo-magnetic nanobeams with geometrical imperfection and different piezoelectric contents", *Microsyst. Technol.*, **25**(9), 3477-3488. https://doi.org/10.1007/s00542-018-4241-3.

Mirjavadi, S.S., Forsat, M., Hamouda, A.M.S. and Barati, M.R. (2019), "Dynamic response of functionally graded graphene nanoplatelet reinforced shells with porosity distributions under transverse dynamic loads", *Mater. Res. Exp.*, **6**(7), 075045.

Mirjavadi, S.S., Forsat, M., Nikookar, M., Barati, M.R. and Hamouda, A.M.S. (2019), "Nonlinear forced vibrations of sandwich smart nanobeams with two-phase piezo-magnetic face sheets", *Eur. Phys. J. Plus*, **134**(10), 508. https://doi.org/10.1140/epjp/i2019-12806-8.

Mirjavadi, S.S., Rabby, S., Shafiei, N., Afshari, B.M. and Kazemi, M. (2017)", On size-dependent free vibration and thermal buckling of axially functionally graded nanobeams in thermal environment", *Appl. Phys. A*, **123**(5), 315. https://doi.org/10.1007/s00339-017-0918-1.

Mohammed, A., Sanjayan, J.G., Nazari, A. and Al-Saadi, N.T.K. (2017). Effects of graphene oxide in enhancing the performance of concrete exposed to high-temperature", *Austr. J. Civil Eng.*, **15**(1), 61-71. https://doi.org/10.1080/14488353.2017.1372849.

Nebab, M., Atmane, H.A., Bennai, R. and Tahar, B. (2019), "Effect of nonlinear elastic foundations on dynamic behavior of FG plates using four-unknown plate theory", *Earthq. Struct.*, **17**(5), 447-462. https://doi.org/10.12989/eas.2019.17.5.447.

Nieto, A., Bisht, A., Lahiri, D., Zhang, C and Agarwal, A. (2017), "Graphene reinforced metal and ceramic matrix composites: a review", *Int. Mater. Rev.*, **62**(5), 241-302. https://doi.org/10.1080/09506608.2016.1219481.

Rafiee, M.A., Rafiee, J., Wang, Z., Song, H., Yu, Z.Z. and Koratkar, N. (2009). Enhanced mechanical properties of nanocomposites at low graphene content", *ACS Nano*, **3**(12), 3884-3890. https://doi.org/10.1021/nn9010472.

Rahmani, M.C., Kaci, A., Bousahla, A.A., Bourada, F., Tounsi, A., Bedia, E.A. and Tounsi, A. (2020), "Influence of boundary

conditions on the bending and free vibration behavior of FGM sandwich plates using a four-unknown refined integral plate theory", *Comput. Concrete*, **25**(3), 225-244. https://doi.org/10.12989/cac.2020.25.3.225.

Refrafi, S., Bousahla, A.A., Bouhadra, A., Menasria, A., Bourada, F., Tounsi, A., ... & Tounsi, A. (2020), "Effects of hygro-thermo-mechanical conditions on the buckling of FG sandwich plates resting on elastic foundations", *Comput. Concrete*, **25**(4), 311-325. https://doi.org/10.12989/cac.2020.25.4.311.

Rezaiee-Pajand, M., Masoodi, A.R. and Mokhtari, M. (2018). Static analysis of functionally graded non-prismatic sandwich beams", *Adv. Comput. Des.*, **3**(2), 165-190. https://doi.org/10.12989/acd.2018.3.2.165.

Safa, A., Hadji, L., Bourada, M. and Zouatnia, N. (2019), "Thermal vibration analysis of FGM beams using an efficient shear deformation beam theory", *Earthq. Struct.*, **17**(3), 329-336. https://doi.org/10.12989/eas.2019.17.3.329.

Sahla, M., Saidi, H., Draiche, K., Bousahla, A.A., Bourada, F. and Tounsi, A. (2019), "Free vibration analysis of angle-ply laminated composite and soft core sandwich plates", *Steel Compos. Struct.*, **33**(5), 663. https://doi.org/10.12989/scs.2019.33.5.663.

Semmah, A., Heireche, H., Bousahla, A.A. and Tounsi, A. (2019), "Thermal buckling analysis of SWBNNT on Winkler foundation by non local FSDT", *Adv. Nano Res.*, **7**(2), 89. https://doi.org/10.12989/anr.2019.7.2.089.

Shamsaei, E., de Souza, F.B., Yao, X., Benhelal, E., Akbari, A. and Duan, W. (2018), "Graphene-based nanosheets for stronger and more durable concrete: A review", *Constr. Build. Mater.*, **183**, 642-660. https://doi.org/10.1016/j.conbuildmat.2018.06.201.

She, G.L., Jiang, X.Y. and Karami, B. (2019), "On thermal snap-buckling of FG curved nanobeams", *Mater. Res. Exp.*, **6**(11), 115008. https://doi.org/10.1088/2053-1591/ab44f1.

She, G.L., Yan, K.M., Zhang, Y.L. *et al*. (2018), "Wave propagation of functionally graded porous nanobeams based on non-local strain gradient theory", *Eur. Phys. J. Plus*, **133**(9), 368. https://doi.org/10.1140/epjp/i2018-12196-5.

Shen, H.S., Xiang, Y., Lin, F. and Hui, D. (2017). Buckling and postbuckling of functionally graded graphene-reinforced composite laminated plates in thermal environments", *Compos. Part B: Eng.*, **119**, 67-78. https://doi.org/10.1016/j.compositesb.2017.03.020.

Soltani, K., Bessaim, A., Houari, M.S.A., Kaci, A., Benguediab, M., Tounsi, A. and Alhodaly, M.S. (2019), "A novel hyperbolic shear deformation theory for the mechanical buckling analysis of advanced composite plates resting on elastic foundations", *Steel Compos. Struct.*, **30**(1), 13-29. https://doi.org/10.12989/scs.2019.30.1.013.

Song, M., Kitipornchai, S. and Yang, J. (2017). Free and forced vibrations of functionally graded polymer composite plates reinforced with graphene nanoplatelets", *Compos. Struct.*, **159**, 579-588. https://doi.org/10.1016/j.compstruct.2016.09.070.

Tlidji, Y., Zidour, M., Draiche, K., Safa, A., Bourada, M., Tounsi, A. and Mahmoud, S.R. (2019), "Vibration analysis of different material distributions of functionally graded microbeam", *Struct. Eng. Mech.*, **69**(6), 637-649. https://doi.org/10.12989/sem.2019.69.6.637.

Tounsi, A., Al-Dulaijan, S.U., Al-Osta, M.A., Chikh, A., Al-Zahrani, M.M., Sharif, A. and Tounsi, A. (2020), "A four variable trigonometric integral plate theory for hygro-thermo-mechanical bending analysis of AFG ceramic-metal plates resting on a two-parameter elastic foundation", *Steel Compos. Struct.*, **34**(4), 511. https://doi.org/10.12989/scs.2020.34.4.511.

Yang, B., Yang, J. and Kitipornchai, S. (2017). Thermoelastic analysis of functionally graded graphene reinforced rectangular plates based on 3D elasticity", *Meccanica*, **52**(10), 2275-2292. https://doi.org/10.1007/s11012-016-0579-8.

Zaoui, F.Z., Ouinas, D. and Tounsi, A. (2019), "New 2D and quasi-3D shear deformation theories for free vibration of functionally graded plates on elastic foundations", *Compos. Part B: Eng.*, **159**, 231-247. https://doi.org/10.1016/j.compositesb.2018.09.051.

Zarga, D., Tounsi, A., Bousahla, A.A., Bourada, F. and Mahmoud, S.R. (2019), "Thermomechanical bending study for functionally graded sandwich plates using a simple quasi-3D shear deformation theory", *Steel Compos. Struct.*, **32**(3), 389-410. https://doi.org/10.12989/scs.2019.32.3.389.

Zhang, L.W. (2017). On the study of the effect of in-plane forces on the frequency parameters of CNT-reinforced composite skew plates", *Compos. Struct.*, **160**, 824-837. https://doi.org/10.1016/j.compstruct.2016.10.116.

Zhu, P., Lei, Z.X. and Liew, K.M. (2012), "Static and free vibration analyses of carbon nanotube-reinforced composite plates using finite element method with first order shear deformation plate theory", *Compos. Struct.*, ***94***(4), 1450-1460. https://doi.org/10.1016/j.compstruct.2011.11.010.

CC